ELSEVIER

Journal of Nuclear Materials 266–269 (1999) 285–290

journal of nuclear materials

# Power deposition in the JET divertor during ELMs

S. Clement *, A. Chankin, D. Ciric, J.P. Coad, J. Falter [1], E. Gauthier, J. Lingertat, S. Puppin

*JET Joint Undertaking, Abingdon OX14 3EA, UK*

**Abstract**

The power deposited in the JET divertor during ELMs has been evaluated using an infrared camera specifically designed for fast measurements. The first results [E. Gauthier, A. Charkin, S. Clement et al., Proc. 24th Euro. conf. on contr. Fusion and Plasma Phys., Berchtesgaden, 1997 (European Physical Society, 1998), vol. 21A, p. 61.] indicated that during type I ELMs, surface temperatures in excess of 2000°C were measured, leading to peak power fluxes in the order of 4 GW/m$^2$. The time integrated power flux exceeded the measured plasma energy loss per ELM by a factor of four. The reasons for this discrepancy are studied in this paper. Redeposited carbon layers of up to 40 μm have been found on the divertor surface in the places where the highest temperatures are measured. The impact of such layers on the power flux evaluation has been studied with numerical calculations, and a controlled simulation of ELM heating has been performed in the JET neutral beam test facility. It is found that neglecting the existence of layers on the surface in a 2D calculation can lead to overestimating the power by a factor of 3, whereas the error in the calculation of the energy is much smaller. An energy based calculation reduces the peak power during type I ELMs to values around 1.2 GW/m$^2$. 

*Keywords:* ELM; Divertor target; Power flux; JET; ITER

## 1. Introduction

Elmy H-mode are being considered as possible operating regimes for ITER. With NBI additional heating it has been shown at JET [1] that all regimes with an acceptable energy confinement have type I ELMs. Sublimation of the graphite tiles due to ELMs is expected to be the main limitation of the operational lifetime of the ITER divertor. It is therefore important to have an accurate assessment of the power load on the divertor in this regime. The first fast IR measurements performed at JET during the MK II divertor experimental campaign showed that during type I ELMs, surface temperatures in excess of 2000°C were measured, leading to peak power densities in the order of 4 GW/m$^2$ [2]. Extrapolations to ITER based on the measured duration of the power deposition and a multi-machine scaling for the stored energy [3] gave an upper limit to the peak power load of 30 GW/m$^2$, for 1 Hz ELM frequency and a duration of 100 μs for the power deposition. Extrapolations from calorimetric measurements from AUG [4] give a value between 0.7 and 1.2 GW/m$^2$, for the same power deposition time.

However, in JET when the energy flux calculated from the IR camera is integrated across the divertor area, it is found that it exceeds the measured plasma energy loss per ELM by a factor of four. The most likely cause for such a discrepancy is related to the possibility of the surface of the tiles being covered with flakes, dust or layers of redeposited carbon that are in bad thermal contact with the bulk material and thus reach higher temperatures than expected. For the power calculation, we use two numerical codes for the heat conduction, KL3b-1D and KL3b-2D (1D and 2D model respectively, with temperature dependent material properties),

* Corresponding author. Tel.: +44 235 464 666; fax: +44 235 464 465; e-mail: sc@jet.uk.

[1] Present address: Département de Recherches sur la Fusion Contre, Association EURATOM-CEA, Centre d'Etudes de Cadarache, F-13108 Saint-Paul-lez-Durance, FR.

0022-3115/99/$ – see front matter 
PII: S0022-3115(98)00530-3

that take into account only the thermal properties of the bulk CFC, as given by the manufacturers (Dunlop, thermal conductivity $k_{xy} = 200$ W m$^{-1}$ K$^{-1}$, $k_z = 60$ W m$^{-1}$ K$^{-1}$ at 300°C). It is also assumed in the calculation that the fibres and the graphite matrix behave in the same way at the surface, although in tiles removed from the divertor after long periods of operation, a different erosion pattern is observed for fibres and matrix. Finally, redeposited layers of plasma facing material are observed on the divertor tiles, as in most machines. At the end of the MK II operational campaign, redeposited layers of carbon and flakes have been found on the divertor tiles [5]. The layers are thicker on the horizontal tile at the inner corner, exactly where the highest temperatures are measured during the ELM. It is, however, very difficult to allow for the presence of a layer in the calculation of the deposited power, since the thickness and thermal properties of the layer are unknown, and are also likely to change with time. In this respect, observations made on the MK I beryllium divertor, in images recorded between discharges, showed a variation of the marks on the tiles on a shot to shot basis [6].

To study how the presence of a layer with lower than bulk thermal conductivity affects the calculation of the power, numerical simulations have been performed. It is found that whereas a large error is made in the calculation of the power, the calculation of the energy is much less affected when an integration is performed over a time that is long compared to the power pulse duration. An energy based calculation of the power has been then tested on data obtained in a controlled experiment in the neutral beam test facility, where a clean divertor tile has been heated by firing an NB source on it. In the light of these results, a new analysis of the infrared camera data obtained during the MK II campaign is presented, and some predictions for ITER are derived.

## 2. The JET IR thermography diagnostic: experimental set-up and first results

The IR camera at JET has been designed to allow fast measurements. It uses a focal plane array of $128 \times 128$ diodes of Cadmium–Mercury Telluride, sensitive in the 3–5 μm range. The camera looks at the divertor from the top of the machine, and provides a 2D image of an area of approximately one square meter or less, depending on the lens used. The spatial resolution is 8 or 4 mm per pixel. The frames are acquired line by line, a complete line being exposed simultaneously. The number of lines used and the number of pixels per line can be fixed before an acquisition, and the ultimate frame rate depends only on the size of the array used. The camera can be clocked at up to 3 MHz. The exposure time can be set independently, from 150 ns to an upper limit set by the read-out time for a line. Typically, for high temperature measurements, an exposure time of 2 μs is used, and line times vary between 13 and 60 μs. These unique features of the camera have been exploited to perform fast measurements during ELMs. Fig. 1, shows an image of the divertor during an ELM. The array is oriented with the lines following the radial (in the figure, horizontal) direction in the divertor. In this way, assuming that the power deposition during ELMs is toroidally symmetric, the vertical direction also represents the time evolution of the temperature at a given radius.

In Fig. 1, the two central bands are the inner and outer strike regions. They are discontinuous in the toroidal direction because the divertor tiles are installed with a pitch to avoid leading edges being exposed, and thus shadow each other. The outermost feature is due to an ELM. During the ELM, a fast (<20 μs) displacement of the strike zones occurs, the power flux moving away from the initial strike zone positions, towards the sides of the divertor. The highest temperatures are measured in the inner side of the divertor region, with temperatures in excess of 2000°C having been recorded. The temperature increases in typically 100 μs. For NB heated discharges with 12–17 MW of additional power, with ELM frequencies from 7–25 Hz, the peak power deposited by an ELM is around 4 GW/m$^2$ [2]. The energy, integrated over the whole divertor area, yields values between 1.2 and 2 MJ, which are larger than the measured stored energy lost by the plasma per ELM by approximately a factor of 4.

## 3. Numerical studies of surface effects in the power calculation

To study the error introduced in our power calculation by considering only the bulk properties of the material, we have used the code ABAQUS [7] to

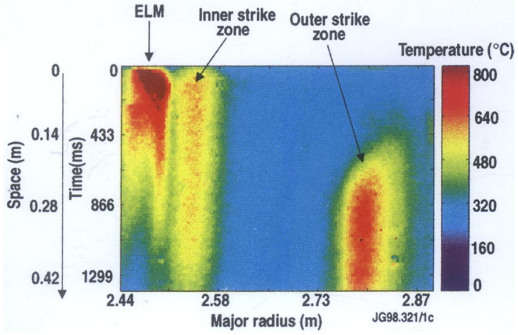


Fig. 1. 2D IR camera image of the divertor during an ELM. The vertical axis represents distance along the toroidal direction, and also time, as the array is exposed line by line from top to bottom in the image.

calculate the temperature evolution of the surface of a tile in the case of layers being present, for a fixed input power. The temperatures are then used to recalculate the power with KL3b-1D. The 1D version (semi-infinite solid with no heat conduction sideways) has been used in this case.

A square pulse of 1.5 GW/m$^2$ lasting 30 μs is the input to ABAQUS (the value of 1.5 GW/m$^2$ is chosen as a reasonable value consistent with the loss in stored energy, but its actual value does not affect the qualitative results). ABAQUS calculates the temperature evolution of a 3.1 cm slab of material (actual thickness of the tile) with the thermal properties of the CFC in the vertical direction. A layer is then added, with a thermal conductivity $k$ layer arbitrarily set at $0.1k_{\text{bulk}}$. Fig. 2(a), shows the temperature evolution obtained in the cases of no layer, and layers of 5, 10, 20 and 40 μm. It can be seen that the surface temperature increases only by 700°C with no layer, but increases very markedly as the thickness of the low conducting layer increases. When these temperatures are fed to the 1D power calculation [Fig. 2(b)], it is immediately apparent that a large error is made if a layer is present, up to a factor of 3 in the case of a 40 μm layer. A close inspection shows that, for the thin layer of 5 μm, there is a large transient spike initially, and a large negative spike in the power after the end of the square pulse. These features disappear as the layer becomes thick enough for its heat conduction to be well described with a 1D model with a lower conductivity. However, in the 40 μm case, small negative powers are found for a long period after the heat pulse. This is more obvious in the energy value, which continues to decrease (and converges towards the true energy value) for long times after the pulse (Fig. 3). In the worst case (40 μm layer), the error in the power is a factor of 3, whereas the error in the energy, integrated over a long time compared to the duration of the heat pulse, is only a 30%. A better evaluation of the power is therefore obtained when the energy, calculated over a long time, is divided by the duration of the power deposition. In the case of ELMs, the duration of the power deposition is measured with a 15% error at the fastest sampling rate. This energy based calculation may be applicable to ELMs, provided that the ELM frequency is low enough to perform a meaningful integration before the next ELM arrives. This calculation has been tested in an ELM simulation experiment where the incident power density was known.

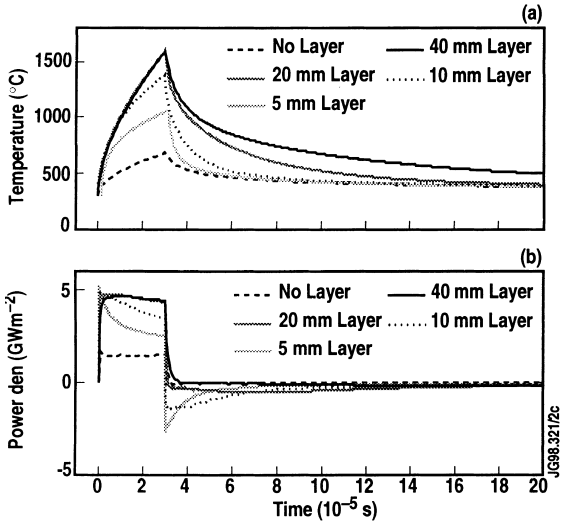


Fig. 2. (a) Temperature evolution calculated by ABAQUS for a square pulse of power flux of 1.5 GW/m$^2$ lasting 30 μs, for the cases: no layer, and layers of 5, 10, 20, and 40 μm thickness, with a thermal conductivity $k_{\text{layer}} = 0.1k_{\text{bulk}}$. (b) Power densities calculated with KL3b-1D, assuming the thermal properties of the bulk material in all cases. The error made by ignoring the existence of a layer increases with the thickness of the layer.

## 4. ELM simulation experiment in the NB test bed

A clean divertor tile has been exposed to repeated short heat pulses delivered by a neutral beam source in the NB test bed facility. (17 ms duration and 42 ms spacing). The surface temperature is recorded with a commercial IR camera. The power density is then measured in situ by removing the tile with a manipulator and firing the beam onto a calorimeter. In this way a power density of 50 MW/m$^2$ is applied uniformly over a spot of 3 cm in diameter. The value of the power is then used as an input to ABAQUS, and the temperature evolution is calculated and compared with the measurements. Fig. 4, shows the experimental and the calculated temperatures (labelled NBexp and HC

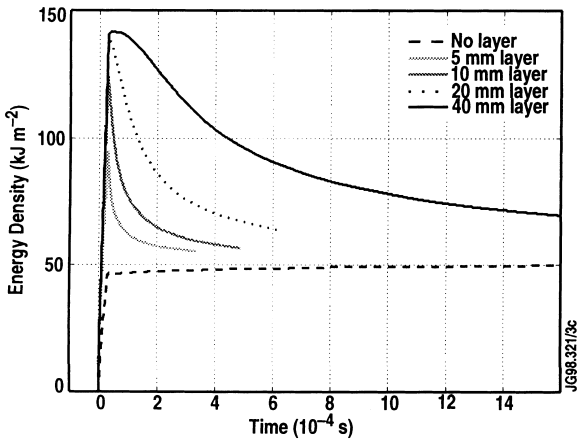


Fig. 3. Energy flux calculated for the cases of Fig. 2(b).

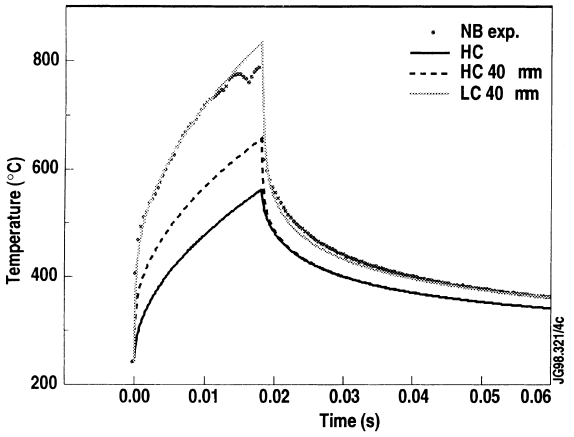


Fig. 4. Neutral beam test bed experiment: time evolution of the temperature for one square heat pulse lasting 17 ms, with 50 MW/m$^2$, in dots. ABAQUS simulations of the temperature for the same heat pulse with the $k_{bulk}$ as given by manufacturer of tiles (label HC), same plus a 40 μm layer with $k_{bulk}/10$ (label HC 40 μm), and for $0.7k_{bulk}$ plus a 40 μm layer with $k_{bulk}/10$ (label LC 40 μm).

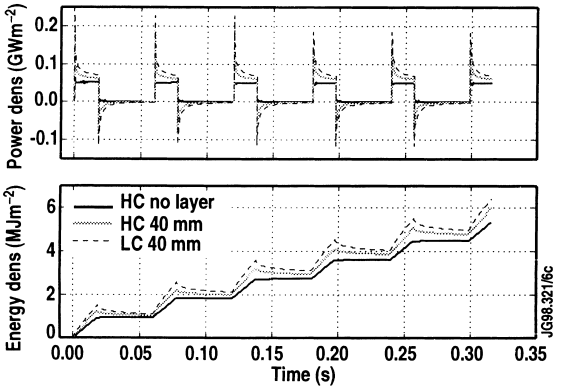


Fig. 5. Power and energy fluxes calculations with KL3b-1D code for the cases described in Fig. 4.

respectively) for the first pulse. It can be seen that the measured temperature shows a marked deviation from the semi-infinite model (bottom curve). In the experimental data, and consistently with previous observations in the NB test bed [8], a fast temperature increase is observed, followed by a slower rise; and after the power is cut off, a correspondingly fast decrease occurs, followed by a slow cooling. These results have been interpreted as due to the presence of powders that sublimate, and are responsible for the fast component of the temperature [8]. The ABAQUS temperature fails to reproduce both the peak values and the cooling curve. When we introduce a layer of 40 μm with a $k_{layer} = 0.1k_{bulk}$ (labelled HC 40 μm in the figure) we modify the peak value of the temperature, but not the cooling part after the initial fast decrease. We conclude that we are not using the right thermal properties of the bulk material. By decreasing the thermal conductivity of the CFC by 30% respect to the values quoted by the manufacturer, we obtain a good match to the cooling curve after the heat pulse (the manufacturer quotes a 20% variation of the thermal properties from tile to tile, and there is a 15% error in the calorimeter measurements). With this new value for $k_{bulk}$, we find that an acceptable match for the temperature evolution is obtained by introducing a 40 μm layer with a $k_{layer} = 0.1k_{bulk}$ (Fig. 4 upper curve). When the temperature curves are fed to the 1D power calculation programme (Fig. 5), we find the expected overestimation for the power values, however, the error in the energy values after 5 heat pulses is only 15%. This result shows that the energy calculation is relatively insensitive to the true nature of the surface coverage, as we know that no redeposited layer is present at the surface of a clean tile. This is an encouraging result for the calculation of the power deposition in the divertor, since the nature of the redeposited layers is unknown, and likely to change with time. However, this calculation relies on integration over a long time, so it will be extremely sensitive to any offset introduced by noise in the temperature signal.

## 5. Application to IR measurements in JET

We have found that the automatic calculation of the temperature from the photon flux measured by the detector does not provide a signal clean enough to allow energy calculations. For each discharge presented, a careful re-calibration of the background and a normalisation of the response has been performed to compensate for the variations in the operating temperature of the detector. The signals for the temperature before and after the cleaning procedure are shown in Fig. 6, where a small difference in the background subtraction causes all the low temperature data to be incorrect. Fig. 7 shows the error that accumulates in the energy calculation in the case of noisy signals.

The discharge #40443 (Fig. 8) is a typical Elmy H-mode at 3 MA/3 T, with 18–16 MW of additional power. The energy and power deposited in the inner corner of the divertor have been calculated in quasi steady state (from 17.5 to 18.4 s, ELM frequency 13 Hz) and during a transient phase after a confinement loss and subsequent recovery (from 21.2 to 22 s, ELM frequency 7 Hz). The energy has been integrated for several ELMs and averaged. In both cases, the average energy density deposited per ELM at the inner corner is ~0.12 MJ/m$^2$. For the measured deposition time of 100 μs, this gives a peak power density value of 1.2 GW/m$^2$ instead

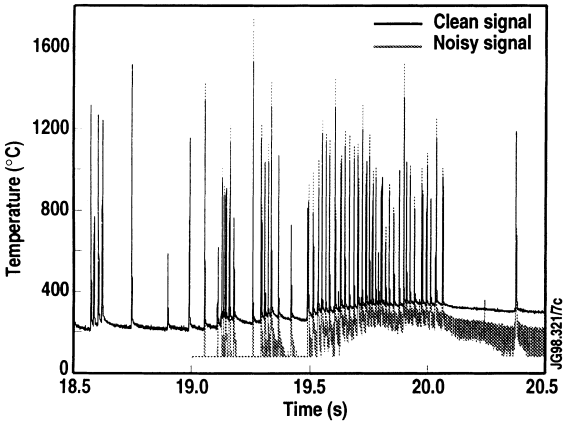


Fig. 6. Time evolution of the surface temperature measured by the IR camera in pulse #40443, at the radius of the ELM before and after the 'special' data cleaning.

of 3.4 GW/m$^2$ (direct power calculation). The estimated energy per ELM deposited in the inner and outer divertor is 0.35 MJ. This value compares reasonably with the average stored energy of the plasma lost per ELM, in this case 0.4 ± 0.15 MJ.

The energy lost per ELM in this discharge is approximately 4.8% of the total plasma stored energy. We can estimate what proportion of the energy deposited by the ELM goes to the zone of maximum heat load in the divertor. The area of this zone is approximately 0.3 m$^2$. In the extrapolation to ITER in [1] it is assumed that all the energy released by an ELM goes to an area of 1 m$^2$, in 100 μs, giving an upper boundary for the power density of 30 GW/m$^2$. The same approach in our case, with 0.4 MJ falling on a 0.3 m$^2$ area in 100 μs, yields 15 GW/m$^2$. This gives a factor of 10 difference with our

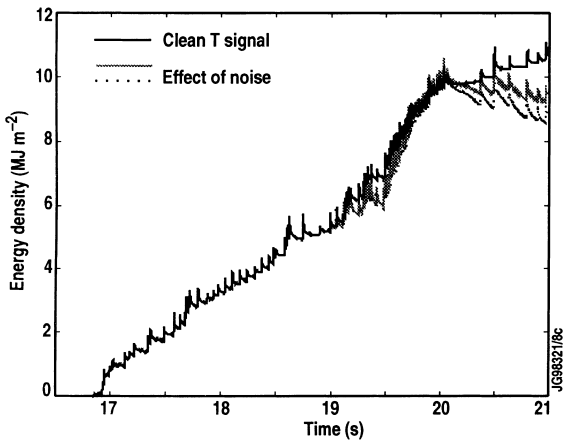


Fig. 7. Energy calculation (KL3b-1D): an example of the errors induced by noisy signals.

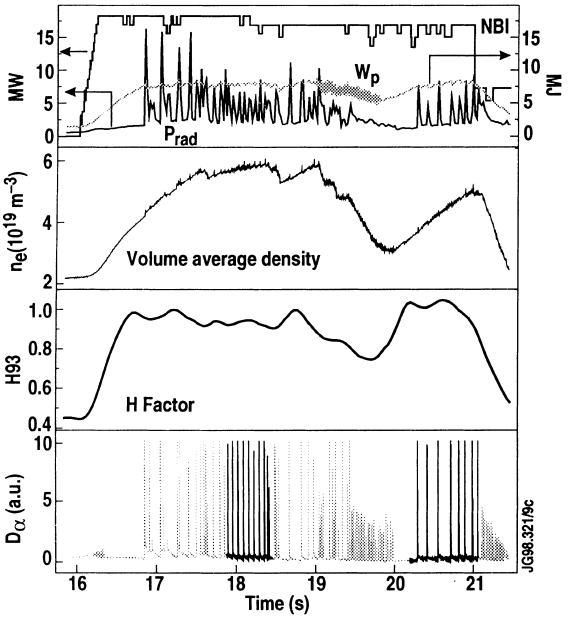


Fig. 8. Time evolution of general plasma parameters for pulse #40443: Total NB injected power, radiated power, stored energy, volume averaged density, enhancement factor H93, $D_\alpha$ at the outer divertor region.

measured peak power load, suggesting that only 10% of the power deposited in the divertor goes to the zone of maximum heat load. The same hypothesis can be made for ITER: the value we obtain depends on the scaling chosen for the power decay length. If we use the design parameter value for the strike zone area, the peak power load is 3 GW/m$^2$, which is within the quoted acceptable value of 0.45 MJ/m$^2$ in 100 μs. However, if we scale linearly the power decay length measured at JET with the radius of the machine, we obtain for ITER a more worrying value of 30GW/m [9].

A high power discharge heated with ICRH (16 MW, H minority, on-axis heating) has been studied for comparison. In this shot, typical ësmallí high frequency ELMs occur during the power ramp-up, followed by type I ELMs at high power, triggered by a sawtooth crash. The high frequency ELMs are too close together to use the energy calculation. However, assuming the same error of a factor of 3 is made, the direct power calculation shows that the deposited power is one order of magnitude lower ($\leqslant 0.1$ GW/m$^2$) than in the NBI case (for $P \approx 12$ MW).

After the sawtooth crash, a short period of type I ELMs is observed. For this shot the camera saturates at 800°C. By comparing the time evolution of the temperature during the ELMs with the NBI case, we estimate that the power deposition is very similar, ~1 GW/m$^2$.

## 6. Summary

Fast IR measurements are essential to study the power deposition during ELMs in a tokamak. With power deposition times of the order of 100 μs, sampling rates of 20 μs are the minimum needed to obtain meaningful measurements. Surface temperatures, however, can be higher than one would expect from the properties of the bulk material when redeposited layers or powder are present. Even in the case of 'clean CFC surfaces', as in the NBI test bed experiment, the peak temperatures measured are still dominated by the presence of ënon bulk materialí, with different thermal properties, on the heat facing surface. However convinced we are of the existence of redeposited layers, these are difficult to include in a model for the power calculation, since their thickness and thermal properties are unknown, and changing in time. The method we propose is to derive powers from the long term calculation of the energy. It has shown to be relatively insensitive to the nature of the coverage of the surface observed (C redeposited layers, powder or even effects due to the differences between fibres and C matrix in CFC) but it relies critically on very clean temperature data and long cool down times between ELMs. It is useful to point out that the high temperatures measured in the divertor are real. The fact that a loose layer is heating up to sublimation temperatures may not be catastrophic for the structural integrity of the divertor plates, but it is a necessary information for impurity studies in the divertor plasma.

## 7. Conclusions

Energy based calculations yield peak powers to the divertor during type I ELMs of ~1.2 GW/m$^2$ during NBI heated discharges. The calculated energy to the divertor deposited during an ELM is consistent with the measured lost plasma energy. Extrapolations to ITER based on these results and a multi-machine scaling lead to a peak power load between 3 and 30 GW/m$^2$. The final value will be critically dependent on the scaling of the power deposition area with the size of the machine.

## Acknowledgements

The help of Dr A. Peacock is gratefully acknowledged. Special thanks are due to Dr G. Saibene.

## References

[1] L. Horton, G. Vlases, P. Andrew et al., Studies of divertors of varied geometry I: non seeded plasma operation, Nucl. Fusion, to be published.
[2] E. Gauthier, I.A. Chankin, S. Clement et al., Proceedings of the 24th Euro. Conf. on Contr. Fusion and Plasma Phys., Berchtesgaden, (European Physical Society, 1998), vol. 21A, 1997, p. 61.
[3] J. Lingertat et al., Proceedings of the 4th Eur. Phys. Workshop, Stockholm, Sweden, 1996.
[4] A. Herrmann, P. Franzen, W. Herrmann, Proceedings of the 24th Euro. Conf. on Contr. Fusion and Plasma Phys., Berchtesgaden, (European Physical Society, 1998), vol. 21A, 1997, p. 1417.
[5] A. Peacock et al., these Proceedings.
[6] J.P. Coad, M. Rubel, C.H. Wu, J. Nucl. Mater. 408 (1997) 241–243.
[7] ABAQUS User Manual, version 5.6-1, Hibbitt, Karlsson and Sorensen Inc.
[8] D. Ciric, H.D. Falter, P. Massmann et al., Fusion Technol. (1994) 391.
[9] D. Pacher, ITER report no. G17 DDD 1 96-08-21, W2.1, Appendix 9, Section 1.7, 1996.